

## Supporting Information

### Color-stable and highly efficient solution-processed white OLEDs with copper(I) complex as a sensitizer

Zhilong Qi<sup>1,2</sup>, Jianlong Xie<sup>1,2</sup>, Qiyin Chen<sup>2</sup>, Shaolong Gong<sup>1,\*</sup> and Guohua Xie<sup>1,2,\*</sup>

<sup>1</sup> Hubei Key Lab on Organic and Polymeric Optoelectronic Materials, Department of Chemistry, Wuhan University, Wuhan 430072, China.

<sup>2</sup> Institute of Flexible Electronics (IFE, Future Technologies), Future Display Institute of Xiamen, Tan Kah Kee Innovation Laboratory, Xiamen University, Xiamen 361102, China.

\*Corresponding addresses: slgong@whu.edu.cn (S.G.) and ifeghxie@xmu.edu.cn (G.X.)

## **Experimental Section**

### **Materials**

All materials were of commercial grade without further purification. The modified hole injection layer, i. e, PEDOT:PSS-HJ-1 was purchased from Jinghang Optoelectronics (Shenzhen) Corporation. Poly(n-vinylcarbazole) (PVK) and the electron injection material lithium 8-hydroxyquinolinolate (Liq) were purchased from Xi'an Yuri Solar Corporation. The electron transporting materials 1,3,5-tri (m-pyrid-3-ylphenyl)benzene (TmPyPB), red phosphorescent material bis(2-methyldibenzo[f,h]quinoxaline)(acetylacetone) iridium(III) ( $\text{Ir}(\text{MDQ})_2\text{acac}$ ), and the hole blocking layer bis[2-(diphenylphosphino)phenyl]ether oxide (DPEPO) were purchased from Luminescence Technology Corporation. The blue TADF material 10,10'-(4,4'-sulfonylbis(4,1-phenylene))bis(9,9-dimethyl-9,10-dihydroacridine) (DMAC-DPS) was synthesized by our group.

### **Photophysical Measurements:**

Hitachi F-4600 fluorescence spectrophotometer and Shimadzu UV-2700 spectrophotometer were adopted to record the PL emission spectra and UV–Vis absorption spectra, respectively. The transient PL decay curves were obtained by FluoTime 300 (PicoQuant GmbH) with a picosecond pulsed UV-LASER (LASER375) as the excitation source.

### **OLED Fabrication and Measurements:**

The pre-patterned Indium-tin-oxide (ITO) coated glass substrates served as the anode. Prior to film deposition, the pre-patterned ITO substrates were cleaned with acetone and ethanol, respectively, and then dried with nitrogen. Later, the substrates were subjected to a 20-minute ultraviolet ozone treatment to enhance the surface work function of ITO. A layer of PEDOT:PSS-HJ-1 was firstly spin-coated onto the ITO substrate to serve as the hole-injecting layer, and then annealed at 120 °C for 10 minutes in a nitrogen-filled glove box. Subsequently, a 50-nm-thick emitting layer (EML) was prepared by spin-coating directly onto the PEDOT:PSS-HJ-1, and dried at 50 °C for 10 minutes. Following this, the devices are transferred to a vacuum deposition system, and

the device structure was completed by thermally evaporating the hole-blocking layer (DPEPO, 10 nm), the electron-transporting layer (50 nm), the electron- injecting layer (Liq, 1 nm) and the aluminum cathode (100 nm) in a vacuum chamber. Before removing the devices from the glove box, all the devices were encapsulated with UV-curable epoxy. Finally, the current-voltage-luminance characteristics and electroluminescent spectra were measured by combining a PR735 SpectraScan Spectroradiometer and a Keithley 2400 source meter unit under ambient condition.

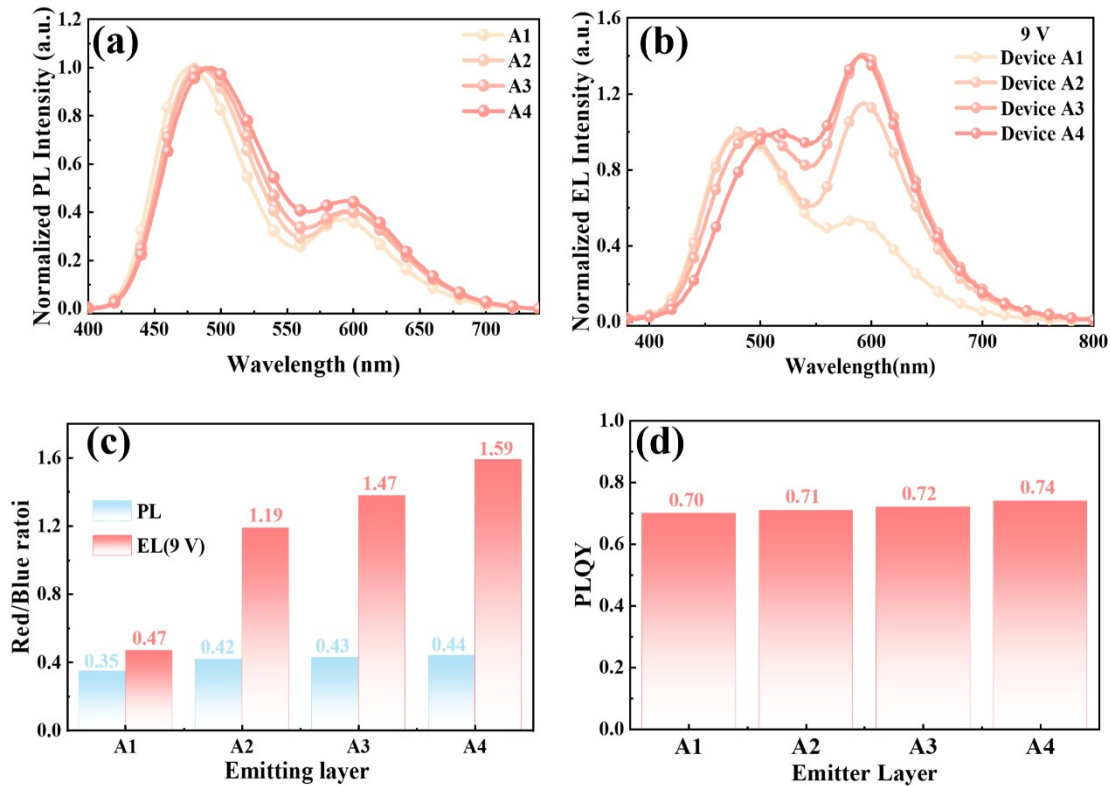


Fig.S1 (a) Normalized PL spectra of film A1, A2, A3 and A4. (b) Normalized EL spectra at an applied voltage of 9 V of devices A1, A2, A3 and A4. (c) The ratios of red/blue components estimated from the PL and EL(9 V) spectrum of the emitting layer based on A1, A2, A3 and A4. (d) The PLQY of the emitting layer based on A1, A2, A3, and A4.

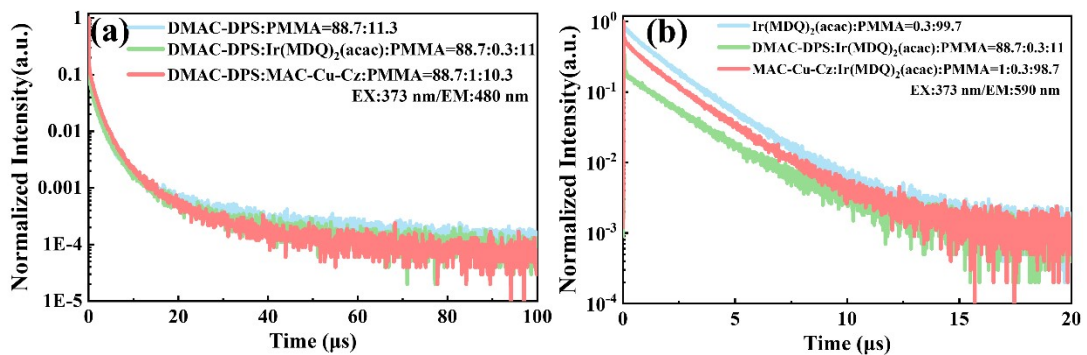


Figure S2 (a) Transient PL decays of the different films composed of DMAC-DPS doped in PMMA observed at 480 nm. (b) Transient PL decays of the different films composed of Ir(MDQ)<sub>2</sub>(acac) hosted by PMMA observed at 590 nm.

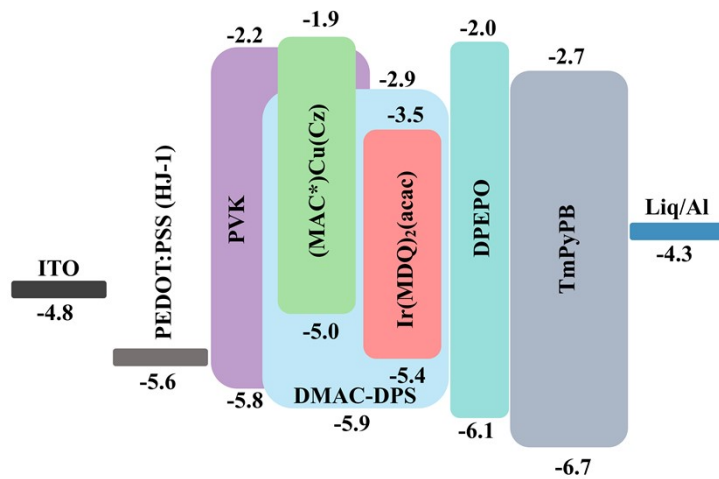


Figure S3 Device structure and the schematic energy level diagram.

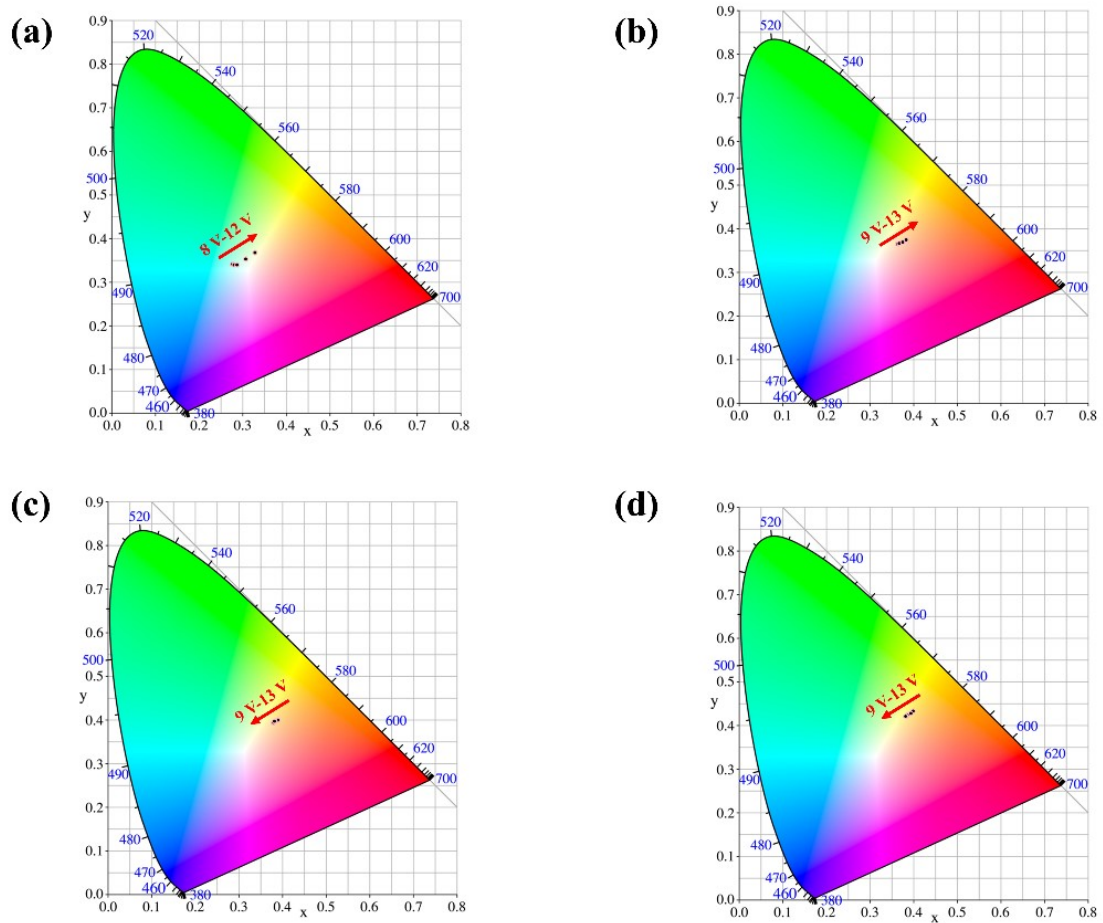


Figure S4 CIE 1931 chromaticity diagram at different driving voltage of the devices A1 (a), A2 (b), A3 (c), and A4 (d).

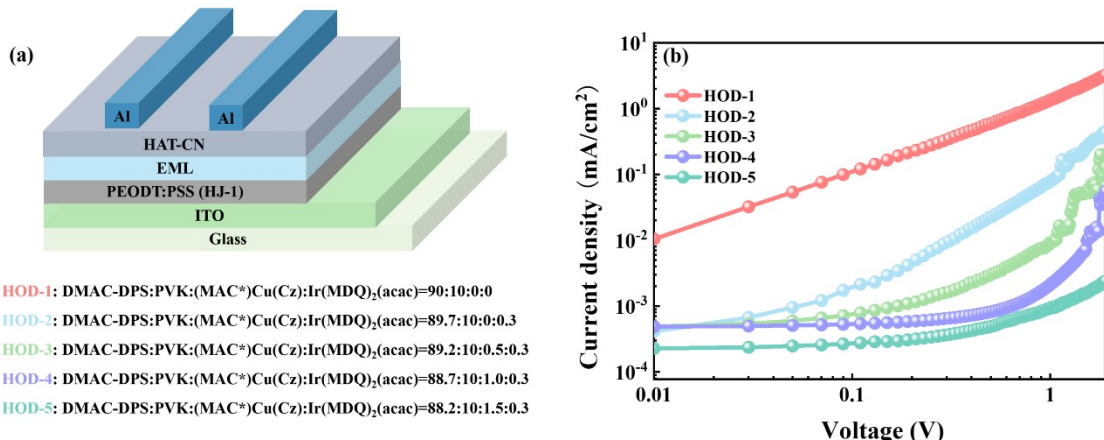


Fig. S5 Device structure (a) and current density curves (b) of the hole-only based on HOD-1, HOD-2, HOD-3, HOD-4 and HOD-5.

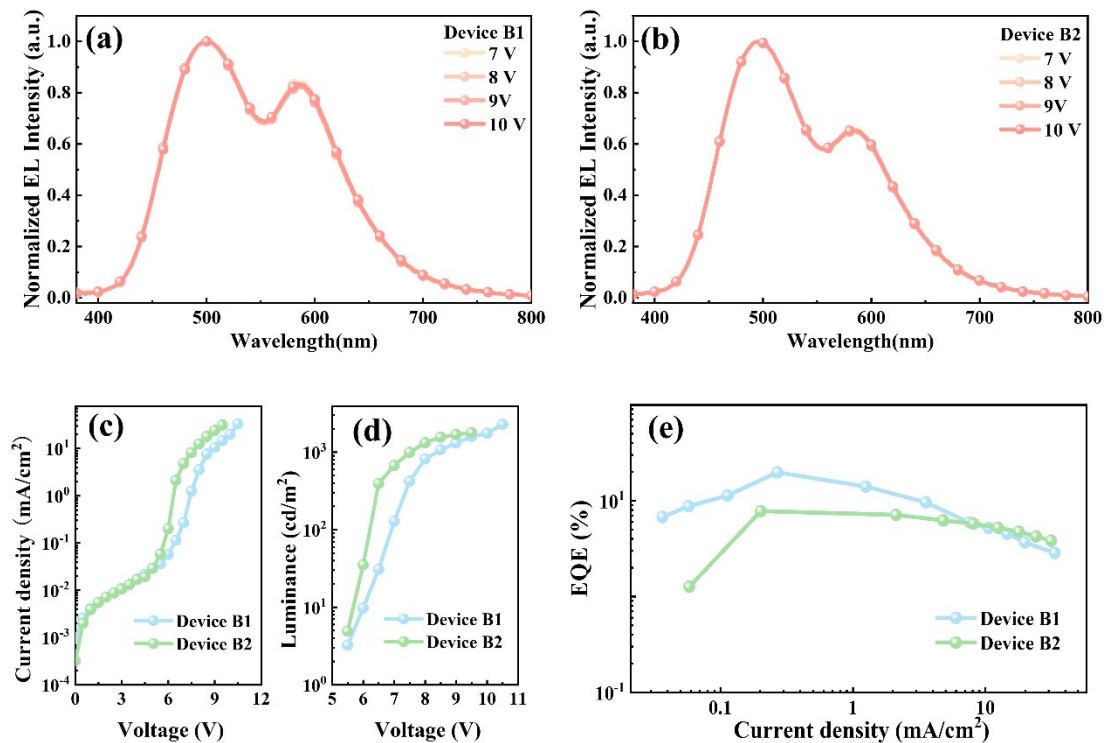


Figure S6 Normalized EL spectra of the devices B1 (a) and B2 (b). (c) Current density-driving voltage curves. (d) Brightness-driving voltage curves, and (e) EQE versus current density curves of the devices B1 and B2, respectively.

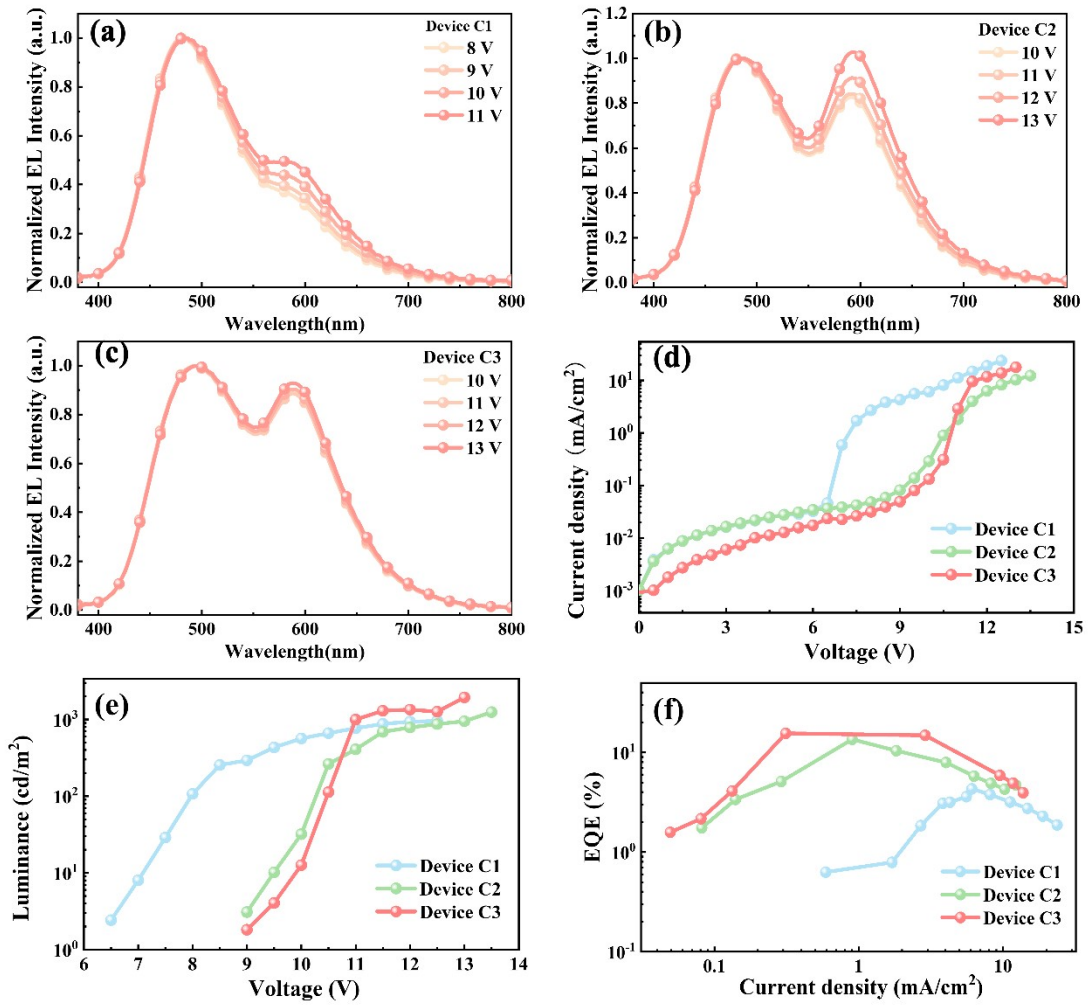


Figure S7 Normalized EL spectra of the devices C1 (a), C2 (b), and C3 (c). (d) Current density-driving voltage curves. (e) Brightness-driving voltage curves, and (f) EQE versus current density curves of the devices C1, C2, and C3, respectively.

Table S1. Detailed computational parameters for Förster radius calculation

	$\Phi_D$	$\kappa^2$	n	$\int_0^\infty F_D(\lambda) \epsilon_A(\lambda) \lambda^4 d\lambda$	$R_0$
$\text{nm}^{-4} \text{M}^{-1} \text{cm}^{-1}$					
<b>DMAC-DPS to</b> <b>Ir(MDQ)<sub>2</sub>(acac)</b>	0.88	0.67	1.7	$3.24 \times 10^{15}$	5.21
<b>DMAC-DPS to</b> <b>(MAC*)Cu(Cz)</b>	0.88	0.67	1.7	$1.84 \times 10^{15}$	4.74
<b>(MAC*)Cu(Cz) to</b> <b>Ir(MDQ)<sub>2</sub>(acac)</b>	0.53	0.67	1.7	$1.60 \times 10^{15}$	4.26

Table S2. Summary of the calculated  $k_{\text{FRET}}$  data.

<b>DMAC-DPS:PVK:</b>				
<b>(MAC*)Cu(Cz):</b>	<b>89.7:10:0:0.3</b>	<b>89.2:10:0.5:0.3</b>	<b>88.7:10:1:0.3</b>	<b>88.2:10:1.5:0.3</b>
<b>Ir(MDQ)<sub>2</sub>(acac)</b>				
<b><math>k_{\text{FRET}} (\text{s}^{-1})</math></b>	$2.15 \times 10^7$	$2.70 \times 10^7$	$5.81 \times 10^7$	$7.60 \times 10^7$

Table S3. Transient photo-physical parameters of the emitting layer consisting of DMAC-DPS:PVK:(MAC\*)Cu(Cz):Ir(MDQ)<sub>2</sub>(acac).

Wavelengt h (nm)	DMAC-DPS:PVK: (MAC*)Cu(Cz):Ir(MDQ) <sub>2</sub> (acac)	A <sub>1</sub>	A <sub>2</sub>	A <sub>3</sub>	τ <sub>1</sub> (ns)	τ <sub>2</sub> (ns)	τ <sub>3</sub> (ns)	τ <sub>d</sub> /τ <sub>p</sub> (μs/ns)
480	89.7:10:0:0.3	16.8	52.7	32.2	13283	2205	527	3.50/8.7
	89.2:10:0.5:0.3	13.6	41.3	19.3	11504	2062	550	3.40/8.3
	88.7:10:1:0.3	8.83	27.2	22.8	11090	1994	647	2.84/6.6
	88.2:10:1.5:0.3	9.3	32.8	31	10930	1823	535	2.44/5.9
590	89.7:10:0:0.3	15	51	147	6324	1071	2072	2.13/-
	89.2:10:0.5:0.3	85	72	7.2	2120	870	17	1.48/-
	88.7:10:1:0.3	67.6	66	6.07	1910	735	15.1	1.27/-

	88.2:10:1.5:0.3	82.8	55.5	6.29	1706	582	16.1	1.20/-
--	-----------------	------	------	------	------	-----	------	--------

Table S4. Transient photo-physical parameters of the different films with DMAC-DPS diluted by PMMA observed at 480 nm and I the different films with Ir(MDQ)<sub>2</sub>(acac) observed at 590 nm.

Wavelengt		<b>Doped film</b>	<b>A<sub>1</sub></b>	<b>A<sub>2</sub></b>	<b>A<sub>3</sub></b>	<b>τ<sub>1</sub></b> (ns)	<b>τ<sub>2</sub></b> (ns)	<b>τ<sub>3</sub></b> (ns)	<b>τ<sub>d</sub>/τ<sub>p</sub></b> (μs/ns)
<b>h</b> (nm)									
480	DMAC-DPS:PMMA=88.7:11.3		47	132.1	41	11600	1780	314	3.60/10.7
	DMAC-DPS: Ir(MDQ) <sub>2</sub> (acac): PMMA=88.7:0.3:11		44.4	127.7	21	10000	1780	208	3.50/9.3
	DMAC-DPS:(MAC*)Cu(Cz): PMMA=88.7:1:10.3		32.1	92	143	12800	907	2690	3.29/5.0
590	Ir(MDQ) <sub>2</sub> (acac):PMMA=0.3:99.7		680	141	2.2	2219	1050	19	2.01/-
	DMAC-DPS: Ir(MDQ) <sub>2</sub> (acac): PMMA=88.7:0.3:11		102	9.74	278	3660	19.02	1792	2.24/-
	(MAC*)Cu(Cz): Ir(MDQ) <sub>2</sub> (acac): PMMA=1:0.3:98.7		577	708	37	2480	1512	412	1.90/-

Table S5 Summary of EL performances of solution-processed WOLEDs of B1, B2, B3, C1, C2, and C3.

<b>Device</b>	<b>V<sub>on</sub></b>	<b>CE<sub>max</sub></b> (cd/A)	<b>PE<sub>max</sub></b> (lm/W)	<b>EQE<sub>max</sub></b> (%)	<b>CIE</b>	<b>CRI</b>
B1	5.4	47.5	21.3	19.8	(0.33, 0.41) <sup>a</sup>	76 <sup>a</sup>
B2	5.2	18.5	9.0	7.8	(0.31, 0.39) <sup>a</sup>	74 <sup>a</sup>
C1	6.5	9.3	2.9	4.3	(0.29, 0.36) <sup>b</sup>	78 <sup>b</sup>
C2	8.8	29.2	8.7	13.6	(0.33, 0.36) <sup>b</sup>	84 <sup>b</sup>
C3	9.0	36.1	10.8	15.6	(0.33, 0.39) <sup>b</sup>	81 <sup>b</sup>

Table S6 Comparison of the EL performance of the reported solution-processed TADF-phosphor hybrid WOLEDs

EML	CE <sub>max</sub> (cd/A)	PE <sub>max</sub> (lm/W)	EQE <sub>max</sub> (%)	CIE (x,y)	CRI	EL spectrum stability	Ref.
G2:Ir(bt) <sub>2</sub> acac	17.69	7.88	10.1	(0.32,0.33))	-	No	<b>1</b>
DczPPy:OXD-7:BPS:Ir(bt) <sub>2</sub> acac	17.34	6.81	6.59	(0.41, 0.41)	73	No	<b>2</b>
mCP:TSPO1:DTPDDA:Ir(MDQ) <sub>2</sub> acac	15.07	5.56	8.40	(0.57, 0.40)	-	-	<b>3</b>
POBPCz:2CzPN:Ir (MDQ) <sub>2</sub> (acac)	29.1	17.2	12.4	(0.36, 0.41)	-	Yes	<b>4</b>
DMAC-TRZ/Ir(dpm)PQ <sub>2</sub>	28.8	18.1	12.32	(0.36, 0.43)	67	No	<b>5</b>
PCz-4CzCN:PO-01	43.1	33.8	19.6	(0.26, 0.39)	-	No	<b>6</b>
CDBP:4CzFCN:Ir(MDQ) <sub>2</sub> acac	-	31.3	20.8	(0.33, 0.39)	-	No	<b>7</b>
Cz-OCzBN:PO-01	45.6	40.9	17.0	(0.34, 0.44)	-	Yes	<b>8</b>
DMAC-TRZ:Ir(dpm)PQ <sub>2</sub> :PO-01-TB	48.7	44.5	17.4	(0.35, 0.44)	-	Yes	<b>9</b>
mCP:TTSA:Ir(MDQ) <sub>2</sub> (acac)	22.46	10.57	11.02	(0.43, 0.39)	72.7	No	<b>10</b>
m-CBP:SpiroAC-TRZ:Ir(MDQ) <sub>2</sub> acac	52.8	33.2	22.9	(0.35,0.39)	80	No	<b>11</b>
mCP:5CzTRZ:Ir(Flpy-CF <sub>3</sub> -EG) <sub>3</sub>	93.2	93.5	31.1	(0.40, 0.47)	-	-	<b>12</b>
mCP: PCzTCFu:Ir(MDQ) <sub>2</sub> (acac)	52.8	31.3	26.7	(0.50,0.39)	-	No	<b>13</b>
4Cz-SO:FIrpic:Ir(MDQ) <sub>2</sub> (acac)	30.4	-	14.5	(0.34, 0.40)		No	<b>14</b>
<b>DMAC-DPS:PVK: (MAC*)Cu(Cz):Ir(MDQ)<sub>2</sub>(acac)</b>	<b>47.8</b>	<b>45.0</b>	<b>21.0</b>	<b>(0.38,0.40)</b>	<b>83</b>	<b>Yes</b>	<b>This work</b>

## References

1. X. Q. Liao, X. Yang, R. Zhang, J. Cheng, J. Li, S. Y. Chen, J. Zhu and L. Li, *J. Mater. Chem. C*, 2017, **5**, 10001-10006.
2. X. Q. Liao, X. Yang, J. Cheng, Y. Li, X. Meng, J. Li, Q. B. Pei and L. Li, *ChemPlusChem*, 2018, **83**, 274-278.
3. C. W. Joo, H. Cho, B. H. Kwon, N. S. Cho, Y. Kim, Y. H. Kim and J. Lee, *J. Ind. Eng. Chem.*, 2018, **65**, 35-39.
4. W. Li, J. W. Zhao, L. J. Li, X. Y. Du, C. Fan, C. J. Zheng and S. L. Tao, *Org. Electron.*, 2018, **58**, 276-282.
5. J. Y. Wu and S. A. Chen, *ACS Appl. Mater. Interfaces*, 2018, **10**, 4851-4859.
6. X. X. Ban, Y. Liu, J. Pan, F. Chen, A. Y. Zhu, W. Jiang, Y. M. Sun and Y. J. Dong, *ACS Appl. Mater. Interfaces*, 2020, **12**, 1190-1200.

7. Z. Y. He, C. Y. Wang, J. W. Zhao, X. Y. Du, H. Y. Yang, P. L. Zhong, C. J. Zheng, H. Lin, S. L. Tao and X. H. Zhang, *J. Mater. Chem. C*, 2019, **7**, 11806-11812.
8. X. X. Ban, F. Chen, Y. Liu, J. Pan, A. Y. Zhu, W. Jiang and Y. M. Sun, *Chem. Sci.*, 2019, **10**, 3054-3064.
9. P. S. Ngo, M. K. Hung, K. W. Tsai, S. Sharma and S. A. Chen, *ACS Appl. Mater. Interfaces*, 2019, **11**, 45939-45948.
10. C. W. Joo, G. Huseynova, J. H. Kim, J. M. Yoo, Y. H. Kim, N. S. Cho, J. H. Lee, Y. H. Kim and J. Lee, *Thin Solid Films*, 2020, **695**, 6.
11. M. M. Lv, W. Zhang, Y. J. Ning, W. Z. Jing, D. D. Song, S. L. Zhao, Z. Xu, L. Fan and B. Qiao, *Adv. Mater. Interfaces*, 2022, **9**, 8.
12. L. Chen, Y. F. Chang, S. Shi, S. M. Wang and L. X. Wang, *Mater. Horiz.*, 2022, **9**, 1299-1308.
13. Q. P. Cao, W. H. Zhang, H. Xu, J. Y. Wang, M. Pei, Y. Q. Qian, T. Zhou, K. Z. Zhang and X. X. Ban, *Chem. Eng. J.*, 2023, **466**, 11.
14. W. H. Zhang, J. M. Yu, Q. P. Cao, Y. Q. Qian, J. Y. Wang, C. X. Yang, H. Y. Zhuang, W. Z. Bian, Y. M. Xin and X. X. Ban, *J. Mater. Chem. C*, 2023, **11**, 16247-16257.